Energetics and fragmentation of single-doped tin and lead clusters

B. Waldschmidt,[1] S. Barman,[2] C. Rajesh,[3] C. Majumder,[4] G. P. Das,[2] and R. Schäfer[1]
[1]*Eduard-Zintl-Institut für Anorganische und Physikalische Chemie, Technische Universität Darmstadt, 64287 Darmstadt, Germany*
[2]*Department of Materials Science, Indian Association for the Cultivation of Science, Jadavpur, Kolkata 700032, India*
[3]*RMC, Bhabha Atomic Research Centre, Mumbai 400085, India*
[4]*Chemistry Division, Bhabha Atomic Research Centre, Mumbai 400085, India*
(Received 6 October 2008; revised manuscript received 27 November 2008; published 27 January 2009)

The fragmentation behavior of the bimetallic cluster ions Sn_NPb^+ and Pb_NSn^+ has been investigated by tandem time-of-flight mass spectrometry in combination with density-functional theory. The low-energy surface-induced dissociation patterns of Sn_NPb^+ and Pb_NSn^+ with $N=6-11$ are dominated by the subsequent loss of atoms. For Sn_NPb^+ first the single lead atom is split off; in contrast the Pb_NSn^+ clusters dissociate mainly in fragments retaining the single tin atom, which is in full accordance with the quantum chemical results. For larger collision energies the complete set of smaller tin fragment ions Sn^+_{N-M} with $M<N$ is found for Sn_NPb^+, whereas the Pb_NSn^+ clusters decay into two series of $Pb_{N-M}Sn^+$ and Pb^+_{N-M} fragments with $M<N$.

DOI: 10.1103/PhysRevB.79.045422 PACS number(s): 36.40.Qv, 31.15.−p, 34.50.−s

In recent decades the properties of clusters became an interesting field of research because clusters allow someone to study the stepwise development of matter from the atom to the bulk. The structural and electronic properties of the group-14 clusters are of particular interest[1–6] because these systems permit someone to study whether the transition from covalent to metallic bonding, which takes place within this group in the bulk, manifests also in reduced dimensions. Additionally the potential of these clusters for applications in nanotechnology is particularly promising. However, not only are the pure element clusters are of interest but also doped or bimetallic cluster species[7–13] because the chemical and physical properties of doped or alloyed clusters may be tuned by varying the composition and the atomic ordering as well as the size of the clusters.

For tin-lead nanoalloys it has been, for example, found that the solubility and the thermal-expansion coefficient depend sensitively on particle size.[14] This behavior has been attributed to a size-dependent cohesive energy. In order to better understand the influence of dopant atoms on the energetics of nanoalloys, we have investigated single-doped tin and lead clusters. In the present paper the surface-induced dissociation of tin-rich Sn_NPb^+ and lead-rich Pb_NSn^+ clusters with $N=6-11$ is analyzed to study the fragmentation behavior of the doped clusters because the unimolecular dissociation of clusters is very sensitive to the binding energies.[15] The comparison of the experimental results with quantum chemical calculations gives deeper insight into the energetics of the single-doped group-14 clusters. After a presentation of the experimental procedure, the results of our quantum chemical calculations will be discussed, followed by a detailed analysis of the experimental data in comparison with the theoretical predictions.

An overview of the apparatus used for the present experiments is already reported in the literature.[16] Therefore, the experiment will be described only briefly.

Bimetallic clusters are produced by a dual laser vaporization cluster source. The cluster source consists of two separate formation zones where homoatomic clusters are generated. These clusters were then transported with the carrier gas to a reaction zone, which allows the formation of alloyed or bimetallic clusters. After that the alloyed cluster helium mixture is expanded through a nozzle into the high-vacuum apparatus, thus generating a molecular beam with isolated clusters.

After passing a double skimmer, positive cluster ions in the molecular beam were accelerated by a collinear Wiley-McLaren-type[17] time-of-flight mass spectrometer (TOF-MS) and detected with a double microchannel plate. Mass spectra[18] were obtained in a linear TOF mode with a 90° electrostatic mirror and mass selection was performed by applying a high-voltage pulse to the mirror.

For the surface-induced dissociation (SID) experiments, the electrostatic mirror was rotated by 90° out of the first position. The mass selected cluster ions were then decelerated between a grounded mesh and the sample hold at an electric potential. The clusters collide with a highly oriented pyrolytic graphite (HOPG) surface if their kinetic energy is high enough. Scattered positive ions were then extracted back by the electric field, which has already decelerated the impinging ions, and were then detected by the double microchannel plate. The collision energy was varied by changing the bias voltage to the sample. In this paper an incident energy E_i stands for the difference between the average kinetic energy of the projectile ions and the potential energy. Since the incident energy spread of the primary ion beam amounts to approximately 150 eV [full width at half maximum (FWHM)],[16,19] fragmentation processes are already observed also for negative values of E_i.

All calculations were carried out using the plane-wave-based pseudopotential approach as implemented in the Vienna *Ab initio* Simulation Package (VASP).[20–22] The electron ion interaction energy and the exchange-correlation functional were described using the projector augmented wave (PAW) (Refs. 23 and 24) and Perdew-Burke-Ernzerhof (PBE) (Ref. 25) schemes, respectively. A large simple-cubic unit cell of side up to 20 Å and the Γ point for the Brillouin-zone integrations has been used. In order to account for the large spin-orbit (SO) coupling effect observed for Pb_N clusters,[26] all the calculations in this work were carried out

 ©2009 The American Physical Society

TABLE I. Binding energies per atom for Sn_NPb and Pb_NSn ($N=1-11$).

N	Sn_{N+1}	Sn_NPb	Pb_{N+1}	Pb_NSn
1	1.18	0.89	0.66	0.89
2	1.71	1.48	1.06	1.24
3	2.15	1.96	1.33	1.54
4	2.31	2.18	1.33	1.52
5	2.50	2.35	1.56	1.73
6	2.62	2.49	1.68	1.83
7	2.55	2.44	1.64	1.78
8	2.63	2.55	1.71	1.84
9	2.69	2.60	1.74	1.83
10	2.63	2.56	1.72	1.83
11	2.64	2.57	1.74	1.84

including the SO effect in the total-energy calculation. A large number of initial structures based on addition (exohedral or endohedral) or substitution by the dopant atom have been generated for each of the Pb_NSn and Sn_NPb clusters to explore the lowest-energy structures.[18]

The binding energies per atom of the lowest-energy isomers of homoatomic and heteroatomic clusters are shown in Table I. It becomes clear from this table that the incorporation of Pb into the Sn_N host cluster reduces the average binding energy per atom compared to Sn_{N+1}. On the other hand substitution of a Pb atom by a Sn atom increases the binding strength.

In order to estimate dissociation energies quantum chemically, we have considered the fragmentation process to occur along the lowest-energy pathways with no additional activation barrier and also entropic effects have been omitted. However, it is expected from statistical rate theory that the lowest-energy pathways dominate the fragmentation behavior because the microcanonical unimolecular rate constants depend sensitively on the dissociation energies.[15] Therefore, we calculated the fragmentation energy for the Sn_NPb and Pb_NSn clusters with $N=6-11$ only by looking at the total energy of the neutral parents and daughters. Within this approach, it is predicted that the Pb_NSn clusters with $N\leq 11$ prefer a monomer evaporation of the Pb atom from the doped cluster. It is also expected that the removal of the Pb atom from Sn_NPb clusters tends to be the most favorable path of fragmentation for $N<11$ while $Sn_{11}Pb$ prefers fission into two large daughter products. It looks as if the evaporation of the Pb atoms seems to be a common lowest-energy fragmentation pathway for both the Pb_NSn and Sn_NPb clusters. However, one has to take into account that experimentally charged clusters have been investigated. Therefore, the ionization potentials of the metal clusters have to be considered for a comparison between theoretical calculations and the experiment. The results predicted theoretically for neutral clusters are summarized together with the experimental observations of charged clusters in Table II.

Surface-induced dissociation has been investigated for Sn_NPb^+ and Pb_NSn^+ ($N=6-11$) clusters on a HOPG surface with collision energies E_i ranging from nominal −300 to 700 eV.[18] In Figs. 1 and 2 the SID patterns of Sn_8Pb^+ and Pb_8Sn^+ in dependence of the incident energy are exemplified.

TABLE II. Comparison between the experimental and the theoretical results for Sn_NPb^+ and Pb_NSn^+ ($N=6-11$). Shown are the dominant dissociation channels.

N	Sn_NPb Theor.	Sn_NPb^+ Expt.	Pb_NSn Theor.	Pb_NSn^+ Expt.
6	Sn_6+Pb	Sn_6^++Pb	Pb_5Sn+Pb	Pb_5Sn^++Pb
7	Sn_7+Pb	Sn_7^++Pb	Pb_6Sn+Pb	Pb_6Sn^++Pb
8	Sn_8+Pb	Sn_8^++Pb	Pb_7Sn+Pb	Pb_7Sn^++Pb
				$Pb_6Sn^++Pb_2$
9	Sn_9+Pb	Sn_9^++Pb	Pb_8Sn+Pb	Pb_8Sn^++Pb
10	$Sn_{10}+Pb$	Sn_{10}^++Pb	Pb_9Sn+Pb	Pb_9Sn^++Pb
11	Sn_6+Sn_5Pb	Sn_{11}^++Pb	$Pb_{10}Sn+Pb$	$Pb_{10}Sn^++Pb$
				$Pb_5Sn^++Pb_6$

In both cases only the parent ions are visible for incident energies E_i up to −20.0 eV/atom. Fragmentation processes occur for $E_i>-20.0$ eV/atom because a part of the cluster pulse is already impinging the surface due to the incident energy spread of approximately 150 eV (FWHM). At low incident energies ($E_i<-5.0$ eV/atom) the subsequent loss of lead and tin atoms is predominately observed, which has

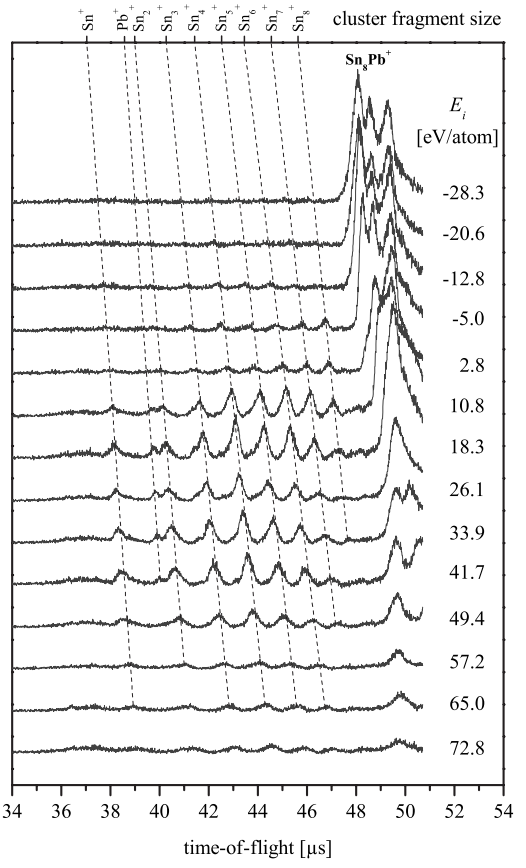

FIG. 1. The incident energy dependence of SID patterns of Sn_8Pb^+. The intensity is plotted against the flight time. On the top the cluster fragment size is assigned.

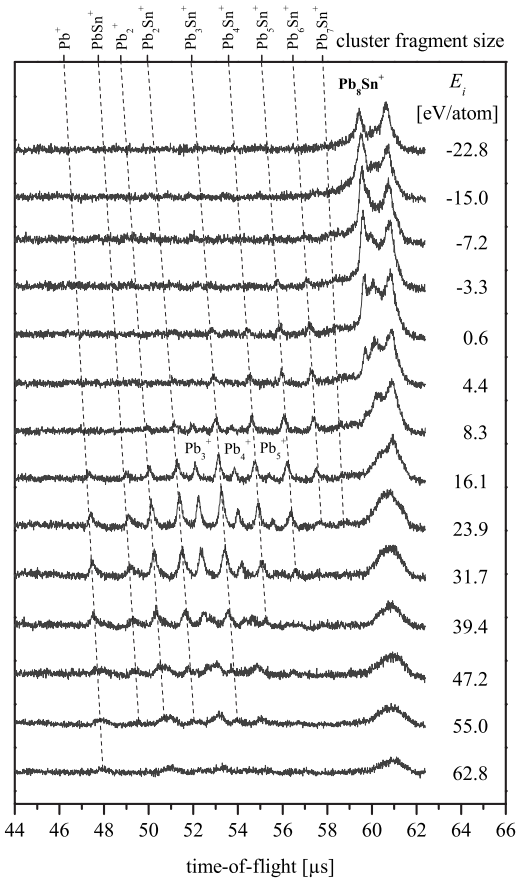

FIG. 2. The incident energy dependence of SID patterns of Pb_8Sn^+. The intensity is plotted against the flight time. On the top the cluster fragment size is assigned.

often been reported in the unimolecular decay of metal clusters.[5,19,27] Increasing the collision energy the fragmentation pattern is shifted toward smaller fragment sizes. At incident energies of ($E_i > 20.0$ eV/atom) the fragment size distribution does not continue to change, but the intensities of the different fragment ions decrease with increasing collision energies due to the importance of implantation processes. For ($E_i > 70.0$ eV/atom) most of the original cluster intensity is vanished.

Comparing the SID spectra of Sn_8Pb^+ and Pb_8Sn^+, it is evident that they behave quite differently. Sn_8Pb^+ first splits off the single lead atom, followed by the fragmentation of the remaining Sn_8^+ fragment. The dissociation of Sn_8^+ takes place by a subsequent loss of tin atoms, which was already described in the literature.[5] Cluster fragments containing the single lead atom as a result of a first loss of tin atoms could not be detected. Within the context of microcanonical unimolecular theories, this indicates that the dissociation energy of the lead atom evaporation is smaller than the fragmentation energies for the loss of tin atoms, i.e., the binding energy of the lead atom is much smaller than the binding energy of the tin atoms, which is in full accordance with the theoretical results.

In contrast the fragmentation patterns of Pb_8Sn^+ consist of two series of signals: one is caused by the loss of the single tin atom resulting in a Pb_8^+ fragment, which further dissociates by the loss of lead atoms.[19] The second observed series results from the first loss of a lead atom, followed by the dissociation of the remaining Pb_7Sn^+ fragment, which itself is the starting ion for two fragment series: one consisting of pure lead cluster fragments and one still containing the single tin atom. Comparing the intensities of these two series, taking the statistical rates of the two fragmentation pathways into account, it is again found that particularly for low incident energies the loss of a lead atom is favored compared to the loss of the single tin atom, indicating that the lead atom evaporation is also for Pb_NSn^+ the fragmentation channel with the lowest energy.

The low incident energy SID spectra for Sn_NPb^+ with $N=6-11$ are also measured.[18] All clusters for $N=6-11$ demonstrate the same fragmentation pattern such as for $N=8$, i.e., the clusters at first split off the single lead atom followed by an evaporation of tin atoms. Therefore, it can be definitely deduced that the lead atom in the tin-rich clusters Sn_NPb^+ with $N=6-11$ is less strongly bounded compared to the tin atoms.

In Table II the experimental results are compared to theoretical predictions. Although only the fragmentation patterns of neutral Sn_NPb clusters ($N=6-11$) are calculated, the experimental results show good agreement with the theoretical results. For all cluster sizes with the exception of $N=11$, the fragmentation channel with the loss of the single lead atom is the one with the lowest dissociation energy. Only for $Sn_{11}Pb$, theory favors the dissociation in Sn_5Pb and Sn_6. However, this discrepancy between experiment and theory can easily be resolved by taking the ionization potentials of the fragments into account. For the neutral clusters the difference of the dissociation energies for the two fragmentation channels, i.e., formation of Sn_5Pb and Sn_6 with respect to the generation of Sn_{11} and Pb, amounts to 0.17 eV. If the ionization potential of Sn_6 or Sn_5Pb compared to Sn_{11} is larger than 0.17 eV, then the Pb atom evaporation channel becomes energetically more favorable for the charged mother ion $Sn_{11}Pb^+$. Experimentally it is found that the ionization potential of Sn_{11} is at least 0.89 eV smaller than that of Sn_6, resolving the observed discrepancy.[6] However, the low-energy SID spectra also show for Sn_NPb^+ clusters with $N>8$ that subunits with four to six tin atoms are rather stable.[18] This is in accordance with the SID behavior of the corresponding pure tin clusters[5] and gives a hint that, for larger tin clusters and probably also for larger Sn_NPb^+ clusters, the fragmentation into stable subunits might be energetically more favorable than the atom loss process. However, in order to clarify this, more experimental and theoretical work is needed.

The low incident energy SID spectra for Pb_NSn^+ with $N=6-11$ are also measured.[18] All clusters with $N=6-11$ demonstrate the same fragmentation pattern. The lead-rich clusters preferentially split off one of the lead atoms instead of the single tin atom. For the low collision energy region, almost no fragments without the single tin atom could be detected. This is in explicit contrast to the tin-rich clusters, which at first eliminate the foreign lead atom.

In Table II the experimental results are opposed with the theoretical predictions. Although only the fragmentation patterns for neutral clusters are calculated, the experimental re-

sults show good agreement with the theoretical results. For all of the investigated species Pb_NSn^+ with $N=6-11$ the atom loss process plays an important role. This is true even if for some clusters the fragment ions $Pb_{N-1}Sn^+$ are hardly resolved in the tail of the mother ion peak. However, for some cluster sizes also fragmentation channels with increased dissociation energy are rather prominent.

For Pb_8Sn^+, the loss of a Pb_2 dimer and, for $Pb_{11}Sn^+$, the decay in cluster fragments of similar sizes, Pb_5Sn^+ and Pb_6, takes place beside the atom loss process with considerable intensity. Both fragmentation channels are the ones with the next lowest predicted dissociation energy. The gap for the decay of Pb_8Sn^+ in Pb_6Sn^+ and Pb_2 amounts to only 0.11 eV, and for $Pb_{11}Sn^+$, the formation of Pb_5Sn^+ and Pb_6 is increased by 0.39 eV compared to the atom split-off channel. In contrast to the tin-rich clusters the importance of these next lowest dissociation energy channels could not be attributed to the fact that experimentally charged clusters have been investigated. Probably the difference in temperature between experiment and theory could be responsible. While during experiment the clusters are produced at finite temperature, theoretically the total-energy calculation under the density-functional theory (DFT) method is done at zero temperature. Moreover, one has to take also into account that the differences of the binding energies are only lower bound for the dissociation energy. Even if one could not exclude that the atom loss process for Pb_8Sn^+ and $Pb_{11}Sn^+$ might require a larger dissociation energy than predicted, it is not clear why this should take place for only these two cluster sizes.

From a comparison of the SID spectra of the bimetallic species with the pure cluster of the same size,[5,19] it becomes clear that the substitution of a lead atom by a tin atom and vice versa does not alter the fragmentation behavior strongly. The most striking feature observed for the bimetallic species is the loss of the single lead atom in the tin-rich clusters, which dominates the SID spectra of Sn_NPb^+ with $N=6-11$. Interestingly, the influence of the substitutional atom seems to be strongest for $Pb_{11}Sn^+$ and $Sn_{11}Pb^+$. Here, the exchange of one of the lead atoms of the homoatomic Pb_{12}^+ cluster by a tin atom increases the formation of rather stable subunits with comparable size, whereas the substitution of a tin atom by a lead atom in the homoatomic Sn_{12}^+ cluster enhances the atom loss process considerably.

We are grateful to Dominic Stranz for his participation in the experiments. We acknowledge financial support by the Deutsche Forschungsgemeinschaft through Grant No. SCHA885/8-1.

[1] J. A. Becker, Angew. Chem., Int. Ed. Engl. **36**, 1390 (1997).
[2] K. LaiHing, R. G. Wheeler, W. L. Wilson, and M. A. Duncan, J. Chem. Phys. **87**, 3401 (1987).
[3] A. A. Shvartsburg and M. F. Jarrold, Chem. Phys. Lett. **317**, 615 (2000).
[4] Ch. Lüder and K. H. Meiwes-Broer, Chem. Phys. Lett. **294**, 391 (1998).
[5] Y. Tai and J. Murakami, J. Chem. Phys. **117**, 4317 (2002).
[6] S. Yoshida and K. Fuke, J. Chem. Phys. **111**, 3880 (1999).
[7] F. Hagelberg, C. Xiao, and W. A. Lester, Phys. Rev. B **67**, 035426 (2003).
[8] J. B. Jaeger, T. D. Jaeger, and M. A. Duncan, J. Phys. Chem. A **110**, 9310 (2006).
[9] V. Kumar, A. K. Singh, and Y. Kawazoe, Nano Lett. **4**, 677 (2004).
[10] S. Neukermans, X. Wang, N. Veldeman, E. Janssens, R. E. Silverans, and P. Lievens, Int. J. Mass Spectrom. **252**, 145 (2006).
[11] C. Rajesh and C. Majumder, J. Chem. Phys. **128**, 024308 (2008).
[12] S. Schäfer and R. Schäfer, ChemPhysChem **9**, 1925 (2008).
[13] R. Ferrando, J. Jellinek, and R. L. Johnston, Chem. Rev. (Washington, D.C.) **108**, 845 (2008).
[14] J.-G. Lee and H. Mori, Eur. Phys. J. D **34**, 227 (2005).
[15] C. Bréchignac, Ph. Cahuzac, J. Leygnier, and J. Weiner, J. Chem. Phys. **90**, 1492 (1989).
[16] M. Turra, B. Waldschmidt, B. Kaiser, and R. Schäfer, Rev. Sci. Instrum. **79**, 013905 (2008).
[17] W. C. Wiley and I. H. McLaren, Rev. Sci. Instrum. **26**, 1150 (1955).
[18] See EPAPS Document No. E-PRBMDO-79-029904 for a mass spectrum, the lowest-energy structures, and further SID spectra. For more information on EPAPS, see http://www.aip.org/pubservs/epaps.html.
[19] B. Waldschmidt, M. Turra, and R. Schäfer, Z. Phys. Chem. **221**, 1569 (2007).
[20] Vienna *ab initio* simulation package, Technische Universität Wien, 1999.
[21] G. Kresse and J. Hafner, Phys. Rev. B **47**, 558 (1993).
[22] G. Kresse and J. Furthmuller, Phys. Rev. B **54**, 11169 (1996).
[23] P. E. Blochl, Phys. Rev. B **50**, 17953 (1994).
[24] G. Kresse and D. Joubert, Phys. Rev. B **59**, 1758 (1999).
[25] J. P. Perdew, K. Burke, and M. Ernzerhof, Phys. Rev. Lett. **77**, 3865 (1996).
[26] C. Rajesh and C. Majumder, J. Chem. Phys. **126**, 244704 (2007).
[27] P. J. Brucat, L.-S. Zheng, C. L. Pettiette, S. Yang, and R. E. Smalley, J. Chem. Phys. **84**, 3078 (1986).